FOUR-QUADRANT SENSORLESS BRUSHLESS ECM DRIVE

R.C. Becerra, GE - MOTORS, Fort Wayne, IN 46801
T.M. Jahns, GE Corporate R&D, Schenectady, NY 12301
M. Ehsani, Texas A&M University, College Station, TX 77843

Abstract **- A four-quadrant brushless Electronically-Commutated Motor (ECM) drive is presented which provides high-quality torque control without discrete current sensors or a rotor position sensor. Rotor position feedback is developed by extracting sufficient information from the motor back-EMF voltage waveforms, and current feedback is provided by current sensors integrated into MOS-gated power switches (MOSFETs or IGBTs). Controller parts count is minimized using a custom VLSI chip which performs the rotor position sensing, PWM current regulation, and various protection functions. The interface between the low-power logic and inverter power switches is accomplished using a High-Voltage Integrated Circuit (HVIC) gate driver for each of the three phase legs. Experimental results using a compact prototype ECM drive card are presented which demonstrate the desired four-quadrant performance without discrete sensors.**

1. Introduction

Rotor position measurement in brushless permanent magnet (PM) motor drives using conventional discrete sensors presents several disadvantages because of the sensor's negative impact on drive cost, reliability, and motor length. The need for additional leads to interconnect sensor and controls is particularly unacceptable in special applications such as compressor drives which require hermetic sealing of the motor inside the compressor unit.

Equivalent rotor position information can be developed without discrete position sensors by processing motor terminal voltage and/or current waveforms. Electronically-Commutated Motor (ECM) drives using PM motors with trapezoidal magnet MMF distributions (also known as brushless DC motor drives) provide attractive candidates for such indirect sensing since only two of the three motor phases are excited at any time instant. As a result, the back-EMF voltage in the unexcited phase can be conveniently measured to provide the basis for determining ECM inverter commutation instants. At least three different algorithms have been reported to accomplish this task, referred to here as the zero-crossing, phase-locked-loop, and back-EMF integration approaches.

The zero-crossing approach [1] is the simplest of the three, and is based on detecting the instant at which the back-EMF in the unexcited phase crosses zero. This zero crossing triggers a timer, which may be as simple as an R-C time constant, so that the next sequential inverter commutation occurs at the end to this timing interval. The price for this simplicity tends to be noise sensitivity in detecting the zero crossing, and degraded performance over wide speed ranges unless the timing interval is programmed as a function of rotor speed.

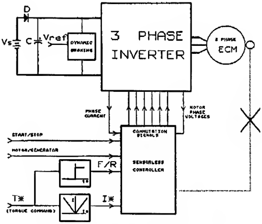

Fig. 1. Four-quadrant sensorless ECM drive block diagram.

An alternative approach [2] uses phase-locked loop (PLL) techniques to lock onto the back-EMF waveform in the unexcited phase winding during each 60 degree excitation interval in order to determine the proper instant for the next inverter switch event. This algorithm is designed to automatically adjust to changes in motor speed.

The third algorithm, referred to as the back-EMF integration approach[3], provides significantly improved performance compared to the basic zero-crossing algorithm introduced above. Instead of using the zero-crossing point of the back-EMF waveform to trigger a timer, the rectified back-EMF waveform is fed to an integrator, whose output is compared to pre-set threshold. The adoption of an integrator provides dual advantages of reduced switching noise sensitivity and automatic adjustment of the inverter switching instants to changes in rotor speed. This algorithm has been implemented in a custom VLSI chip together with current regulation, drive protection, and mode control logic for use in production ECM drives.

One of the special problems faced by any ECM

CH2992-6/91/0000-0202 $1.00 © 1991 IEEE

indirect position sensing scheme using back-EMF waveforms is low-speed performance. The basis for this problem is easy to appreciate since the back-EMF amplitude is proportional to rotor speed, thereby dropping to zero at rotor standstill. Choice of pulse-width-modulation (PWM) technique to achieve the current regulation plays an important role in determining the minimum speed at which the indirect position sensing algorithm will function. Development of the custom VLSI ECM controller chip mentioned above has made it possible to coordinate the PWM current regulation and position sensing in the best possible manner to enhance low-speed performance.

Regulation of the motor phase currents is crucial in any high-performance ECM drive since it provides the basis for instantaneous torque control. Techniques for overcoming the limitations of resistive shunt current sensors by using current sensors integrated into the inverter power switches have been described in a previous paper [4]. The introduction of these integrated current sensors in combination with High Voltage Integrated Circuit (HVIC) gate drivers provides multiple system advantages including elimination of discrete current sensors, improved protection, and reduced controller parts count.

This paper describes a new four-quadrant ECM drive which combines the advantages of indirect rotor position sensing and current sensor integration to provide high-quality drive performance without discrete sensors. The combined use of a custom VLSI controller chip, HVIC gate drivers, and power MOSFETs with integrated sensors provides the basis for a compact, robust drive without sacrificing performance. Experimental results gathered from a prototype "sensorless" ECM drive are provided to illustrate system performance during both motoring and regenerating operation.

2.

2.1 Basic ECM Operation

It is assumed that the reader is already acquainted with the fundamentals of ECM drive operation [5,6] so that only a highly condensed summary is presented here. The subject of this work is a three-phase ECM drive configuration using a six-switch full-bridge inverter. The back-EMF of each motor phase is approximately trapezoidal with two 120 degree intervals of constant voltage (+E and -E), and the amplitude E is proportional to rotor speed.

position information is used to sequentially change the "active" inverter switch pairs six times each electrical cycle in order to continually synchronize the phase excitation with the magnet MMF wave. As a result of this synchronization, the developed motor torque T is proportional to the phase winding current I. Polarity of the torque is reversed by reversing the direction of current flow through the two active windings. The ECM can thereby operate as a motor or generator in both directions of rotation, providing the basis for four-quadrant operation.

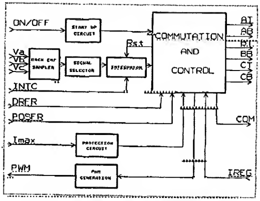

Fig. 2. Functional block diagram of the Universal ECM controller chip.

2.2 ECM Drive Configuration

Figure 1 shows a block diagram of the new four-quadrant ECM drive including both indirect rotor position sensing and integrated current sensing. The 3-phase inverter block uses six power MOSFETs with integrated current sensors and three HVIC phase-leg drivers, similar to the configuration described in [4]. The controller block has responsibility for determining the instantaneous rotor position using information extracted from the motor terminal voltages which are fed to it as shown in Fig. 1. In addition to determining the "commutation" instants between inverter switches, the controller also regulates the motor phase current using the applied torque (i.e., current) command combined with feedback information from the integrated current sensors.

The drive shown in Fig. 1 is designed to operate in all four quadrants of the torque-speed plane. The relationship between back-EMF, current, torque, and speed can be summarized by the following equation specified here for one of

$$T_a(t) = \frac{E_a(t)\ I_a(t)}{n} \qquad (1)$$

spective , the back-EMF voltage and current in the phase A winding, $T_a(t)$ is the torque contributed by phase A (in Nm), and n is the rotor speed (in rad/s).

Referring to Eqn. (1) above, the drive system operates as a motor whenever the back-EMF and phase

current share the same polarity, forcing the developed torque and rotor speed to likewise share the same polarity. Electric power fed from the supply V_s is converted into mechanical output power under such motoring conditions. Conversely, the drive operates as a generator (or, equivalently, as a brake) whenever the back-EMF voltage and phase current have opposite polarities, so that mechanical power from the load is converted back into electrical power. If the electric power supply is not designed to accept this returned power, the drive must include a either a storage capacitor of sufficient size to store the excess energy or a dynamic braking circuit (as shown in Fig. 1) to dissipate it.

The controller block in Fig. 1 controls both the amplitude and polarity of the developed torque. The operator torque command T^* is converted into the motor phase current command I^* by means of the absolute value function block shown in Fig. 1, thereby setting the amplitude of the regulated current through the motor windings. The direction of current flow through these windings is determined by the polarity of the torque command which is also extracted and delivered to the controller.

3. Controller Operation

The controller block in Fig. 1 performs two key functions in order to achieve the desired torque control. These include both indirect rotor position sensing using measured back-EMF waveforms, and current regulation using feedback information from the integrated current sensors imbedded in the inverter power switches. A description of each of these major functions is provided in the following sections.

3.1 Indirect Rotor Position Sensing

Rotor position sensing is accomplished using the back-EMF integrator algorithm [3] briefly introduced in Section 1. This sensing scheme has been implemented in a proprietary custom-VLSI controller chip which GE now uses in the majority of its production ECM drives. A simplified block diagram of this 28-pin Universal ECM (UECM) controller chip is provided in Fig. 2.

Although the UECM accomplishes a variety of controller functions, discussion in this section will focus on the means of achieving the desired rotor position sensing. Since the back-EMF voltage amplitudes can be very large compared to the logic supply voltage, an external resistive divider circuit delivers scaled versions of the three motor phase voltages to the UECM chip. The neutral voltage of the wye-connected motor windings is artificially generated inside the chip in order to develop measurements of the three phase-to-neutral voltages. The signal selector block shown in Fig. 2 is responsible for selecting the phase-to-neutral motor voltage of the unexcited winding. This selected phase voltage equals the desired back-EMF voltage needed for position sensing as soon as the residual inductive current flowing in the unexcited winding immediately following the removal of excitation decays to

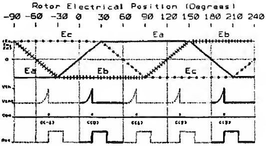

Fig 3. Key waveforms illustrating operation of indirect position sensing including the idealized back EMF waves (Ea, Eb, and Ec), the integrator output ($Vint$), the commutation instants (Com), and the reset interval (Rst).

zero. The controller includes special provision to insure that the position sensing is unaffected by these residual currents, as described in more detail below.

The waveforms sketched in Fig. 3 help to explain the operation of the position sensing algorithm. The integrator block in Fig. 2 consists of an analog integrator which begins to integrate the selected back-EMF voltage (or more precisely, its absolute value) as soon as the back-EMF crosses zero, developing the signal $Vint$ shown in Fig. 3. The shape of this $Vint$ signal can be appreciated from the fact that the instantaneous back-EMF voltage is varying approximately linearly with time in the vicinity of the zero-crossing, so that

$$E(t) = E_0\, t$$

$$Vint = \int_0^t \frac{E(t)}{k}\, dt$$

$$Vint = \frac{E_0\, t^2}{2k} \tag{2}$$

where k is the integrator gain constant. The instant of the next commutation event occurs when $Vint$ reaches a pre-set fixed threshold voltage Vth. Since the amplitude of the back-EMF (Eo in the above equation) is proportional to speed, the conduction intervals automatically scale inversely with speed with a fixed threshold voltage Vth. As shown in Fig. 3, the integrator is reset by signal Rst. The width of the Rst reset pulse is set to insure that the integrator can never start integrating until the residual current in the unexcited phase has decayed to zero.

The choice of threshold voltage Vth and integrator constant k for a given motor determines the specific alignment of the phase current excitation waveform with the back-EMF voltage. Varying Vth or k has the effect of varying this current-voltage waveform alignment, measured in terms on an advance angle. If perfect alignment corresponds to zero advance angle, it has been shown previously [7] that moderate increases in this advance angle (e.g., by reducing k in Eqn. 2 above) can be used to force faster phase current build-up in order to develop extra torque at high speeds. However, it has been

suggested in [5] that an advance angle of approximately 10 elec. degrees provides a good compromise between high-speed torque production and low-speed torque-per-Amp efficiency.

As mentioned earlier, low-speed operation require special provisions since the back-EMF drops to zero at standstill. For motor start-up, an oscillator sequentially steps the commutation state machine at a fixed rate in the desired direction of motor rotation, energizing two of the three motor phases during each interval. As soon as the rotor moves in response to this open-loop stepping sequence, the integrator of the position detection block in Fig. 2 starts integrating the back-EMF voltage from the unexcited phase. When the motor speeds up sufficiently so that the integrator reaches its threshold level before the next open-loop step, the start-up oscillator is automatically overridden so that the back-EMF sensing scheme smoothly takes over control of the inverter switch commutation sequencing.

Since motor back-EMF amplitude varies directly with rotor speed, the indirect position sensing scheme is particularly sensitive at low speeds to noise generated by inverter switching during PWM current regulation. In order to minimize this sensitivity, a special PWM technique has been implemented which permits good tracking of the rotor position down to speeds of a few r/min. The purpose of this technique is to extinguish the current in the phase windings at the end of each 120 degree conduction interval as quickly as possible. By doing so, the terminal voltage of the unexcited winding becomes useful for back-EMF sensing as soon as possible following the off-commutation of the phase. This objective is accomplished by shifting responsibility for PWM switching among the six inverter switches in a specific sequence. It is based on the fact that, at any time instant during motoring operation, only one of the two active inverter switches must execute the PWM switching for current regulation while the second switch is held in its "on" state [4].

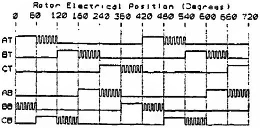

Fig. 4. Commutating signals for the inverter switches showing a preferred PWM sequence for fast current decay in the off-going phase. (AT=Phase A upper switch, AB=Phase A lower switch, etc.)

The preferred sequence for shifting this PWM responsibility is sketched in Fig. 4 (Note that this technique applies only during motoring operation, as discussed below in Section 3.3.) Each of the six switches is active for an interval of 120 electrical during each cycle (signified by either a high or chopped logic level in Fig. 4), and this active interval can be separated into two 60 degree intervals. As shown in Fig. 4, each switch is held in its "on" state during the first of these two active intervals and executes PWM switching during the second interval, as signified by the high-frequency chopping. This scheme meets the criterion of one (and only one) active PWM switch at all times. Using this sequencing technique, the free-wheeling current in the off-going phase is driven to zero more quickly than if the new on-going phase immediately enters PWM operation. This sequencing technique also has the beneficial effect of distributing the PWM switching operation evenly among all six inverter switches during the course of the cycle.

3.2 Current Sensing Configuration

As mentioned in the Introduction, motor phase currents are measured using current sensors integrated into the MOS-gated inverter power switches. A block diagram of the inverter power state showing the current feedback configuration is provided in Fig. 5. The basic principles associated with this inverter configuration, including the use of HVIC phase-leg gate drivers and integrated current sensors, have been presented previously [4] and will not be repeated here. However, the specific sensor configuration sketched in Fig. 5 includes important changes which deserve explanation.

Unlike the drive control scheme presented in [4] which uses the HVIC gate drivers to perform the current regulation control individually for each phase, the new system uses the built-in control features of the UECM chip to perform this regulation control for all three phases. Motor current feedback information is derived from sensed current measurements in the three lower inverter switches, S4, S5, and S6 in Fig. 5. Specifically, the current sense signals from these three lower switches, marked Ia', Ib', and Ic' in Fig. 5, are tied together at the sensing resistor R_s which develops the single feedback signal V_{sense} representing the motor current. This simple hard-wire connection is sufficient for this particular drive since only one lower switch conducts the motor current at any time instant, and the sense leads behave as paralleled current sources. That is, the sense leads for the two lower switches that are not conducting do not interfere with current measurement in the conducting switch because they present high impedances at the R_s node point.

The three upper switches in the inverter configuration of Fig. 5 also incorporate integrated current sensors, although information from these sensors is not used to perform the phase current regulation. Instead, these upper switch current measurements are used only for overcurrent protection which is executed in the associated HVIC driver chips as described previously in [4].

One important constraint imposed by the integrated current sensors is that the associated current switch can only provide useful current feedback information only when the switch is conducting. If a lower switch is performing PWM switching during any interval (see Fig.

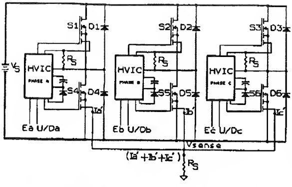

Fig. 5. Simplified circuit schematic of the 3-phase inverter showing the basic elements of the HVIC driver and the composite current from the integrated current sensors of the lower three power devices.

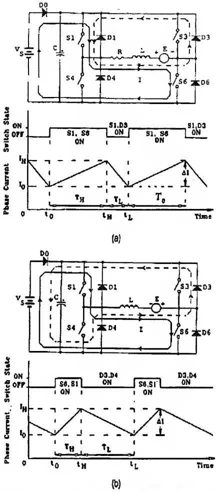

Fig. 6. Equivalent circuit for motor drive phases A and C and steady-state waveforms for fixed-frequency current regulation showing one PWM cycle of phase current and gate drive signal. (a) Motoring. (b) Regeneration.

4), current feedback to the UECM chip is lost whenever the lower switch is turned off. This temporary loss of current feedback information must be specially accommodated by the current regulation algorithm implemented in the UECM chip as described in the next section.

3.3 Current Regulation Algorithm

In order to extract the best possible drive performance, the current regulator operates differently during motoring and regenerating (braking) operation. These differences are highlighted using the simplified inverter diagrams and waveforms in Fig. 6 focussing on the interval when phases A and C are active. The two energized motor phases are modeled as an equivalent inductance L and resistance R in series with back-EMF voltage E. As shown in Fig. 6a, only one switch (S6) is actively involved in PWM operation during motoring operation, while the other active switch (S1) is held on throughout the interval [4]. It should be noted that either S1 or S6 could serve equivalently as the active PWM switch during this interval of motoring operation.

In comparison, braking operation during the same interval shown in Fig. 6b uses both S1 and S6 as simultaneous PWM switches in order to regenerate motor energy back to the source [8]. Note that the polarity of the effective back-EMF source E is reversed in the process of changing from motoring to regeneration. The resulting current waveforms shown in Figs. 6a and 6b have similar sawtooth waveshapes (low motor resistance R is assumed, yielding the piecewise linear waveforms), but the current ripple characteristics are quite different as described below.

Only certain classes of current regulation algorithms are eligible for this drive application because of the incomplete current feedback constraint which is imposed by the use of integrated current sensors as noted in Section 3.2. One particular algorithm referred to as the "constant off-time" current control scheme has been discussed previously in [4]. The UECM chip executes a related but different algorithm known as the "constant-frequency" control which, as the name implies, holds the PWM frequency constant. Referring to motoring waveforms in Fig.6a, the PWM frequency period T_0, represented by the sum of on-time T_H and off-time T_L, is held fixed each cycle. The PWM switch S6 is held "on" until the switch current (which is being fed back to the control) reaches the commanded current threshold I_H, at which time S6 is opened. S6 then remains "off" until the end of the fixed T_0 period, at which time it closes again to begin the next PWM cycle. Operation of this constant-frequency algorithm is exactly analogous during

regenerative operation in Fig. 6b., except that both S1 and S6 are opened when the current reaches I_H.

Motoring Operation

Equations for the instantaneous motor phase current waveforms during steady-state PWM motoring operation can be conveniently derived using the simplified equivalent circuit shown in Fig. 6a. During the interval when both switches S1 and S6 are "on", the motor current $i(t)$ rises according to:

$$i(t) = \frac{V_s - E}{R}\left[1 - e^{-\frac{t}{\tau}}\right] + I_0 e^{-\frac{t}{\tau}} \qquad (3)$$

where $\tau = L/R$ and I_0 is the initial current at the beginning of the interval $(t = t_0)$. Switch S6 is turned off when the rising motor current reaches threshold I_H so that the free-wheeling motor current flowing through S1 and diode D3 decays according to:

$$i(t) = \frac{E}{R}\left[e^{-\frac{t}{\tau}} - 1\right] + I_H e^{-\frac{t}{\tau}} \qquad (4)$$

The amplitude of the current ripple varies as the amplitude of the back-EMF voltage E varies. The steady-state amplitude of this current ripple Δi during motoring operation with constant-frequency current regulation has been derived for the simplified case of zero motor resistance. This condition of $R = 0$ represents a useful approximation for many practical situations. The resulting current ripple is expressed as a function of the normalized back-EMF voltage, E/V_s, as follows:

$$\Delta i = \frac{V_s T_0}{L}\left[1 - \frac{E}{V_s}\right]\frac{E}{V_s} \qquad (5)$$

Figure 7 plots this expression for motoring operation, showing that the current ripple amplitude has a maximum value of $V_s T_0/4L$ when the back-EMF voltage is one-half of the source voltage (approximately half of rated speed).

Regenerative Braking Operation

Similarly, instantaneous current waveforms can be derived for PWM braking operation using the circuit conditions of Fig. 6b. Following the time instant t_0 when both switches S1 and S6 are turned "on", the motor current rises according to:

$$i(t) = \frac{V_s + E}{R}\left[1 - e^{-\frac{t}{\tau}}\right] + I_0 e^{-\frac{t}{\tau}} \qquad (6)$$

This current expression has a very similar form to that of the rising current during motoring operation in Eqn. 3 above, except that here the back-EMF polarity aids the source voltage in driving the motor current upward more rapidly.

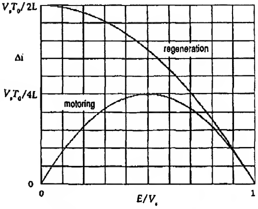

Fig. 7. Current ripple vs. normalized back EMF for motoring and regeneration.

When switches S1 and S6 both open at time t_H in Fig. 6b, the motor current falls as energy is fed back to the inverter bus. If the power source cannot accept this regenerated power (as indicated by the diode D0 in Fig. 6b), the bus capacitor C must accept the energy for temporary storage. Assuming that the motor resistance R is quite small, the resulting second-order system causes the motor current to decay according:

$$i(t) = -\frac{(V_s - E)}{\omega L} e^{-\alpha t}\sin(\omega t) + \frac{\omega_0}{\omega} I_H e^{-\alpha t}\sin(\omega t - \theta) \qquad (7)$$

where $\alpha = R/2L$, and $\omega_0 = 1/\sqrt{LC}$, $\theta = \tan^{-1}(\omega/\alpha)$, and $\omega = (\omega_0^2 - \alpha^2)^{1/2}$.

In practice, a bus storage capacitor may not be sufficient to handle the regenerated energy without the bus voltage building up to unacceptably high levels. In that case, a dynamic brake circuit is often connected across the input supply bus as shown in Fig. 1 to dissipate the extra energy. This circuit will then be controlled as a shunt voltage regulator to draw off the extra capacitor charge until the elevated bus voltage is reduced back to its nominal value of V_s.

An expression for the current ripple with constant-frequency current regulation has been derived for braking operation under the simplifying assumptions of zero motor resistance and fixed source voltage V_s (e.g., large C). The resulting expression for Δi is given as follows:

$$\Delta i = \frac{V_s T_0}{2L}\left[1 - \left(\frac{E}{V_s}\right)^2\right] \qquad (8)$$

When plotted on Fig. 7, one notes that the peak current ripple for regenerative operation is twice the maximum

value during motoring operation, and occurs at standstill ($E = 0$).

4. Drive Implementation

A "sensorless" ECM drive system for a 0.5 hp machine has been designed, built, and tested using integrated current sensors and indirect rotor position sensing as described in this paper. More details regarding the implementation of the controller section of the drive (see Fig. 1) are provided in Fig. 8.

At the heart of this controller is the UECM control chip. The UECM chip's role in performing the indirect rotor position sensing was discussed earlier in Section 3.1. In addition, it executes the constant-frequency PWM current regulation algorithm and enforces the preferred PWM switch sequence shown in Fig. 4. The ECM torque polarity is controlled by the UECM chip on the basis of the DRFR input, while the POSFR input informs the UECM chip of the direction of rotation. Referring back to Fig. 2, the UECM chip is also designed to execute the necessary start-up sequence as well as to provide over-current shut-down protection.

The interface between this UECM chip and both the operator commands and inverter power stage is concentrated in a programmable logic array labeled as PLA in Fig. 8. A major portion of the digital logic implemented in this PLA is devoted to translating the format of inverter switch commands delivered by the UECM chip (top-bottom format) to the input format required by the Harris CS601 HVIC driver chips (up/down-enable format) [9]. However, the second major function of the PLA is to control the operating quadrant of the drive, including transitions between motoring and regenerative operation, and between forward and reverse rotation. In particular, the PLA is responsible for enforcing the change between motoring operation with one active PWM switch (Fig. 6a), to regenerative operation with two active PWM switches (Fig. 6b). In addition, the PLA develops the POSFR and DRFR input commands needed by the UECM chip to keep track of the operating quadrant.

As mentioned earlier in Section 2, the relative polarities of the motor's torque and speed determine whether the drive system is motoring or regenerating. For example, if the motor torque has negative polarity, the drive system changes from regenerating to motoring operation as the motor speed passes through zero speed from positive to negative polarity rotation during a speed reversal. As a result, speed is a significant system variable for controlling the drive's operating quadrant. Since the ECM has no shaft-mounted speed sensor, a speed detector circuit is included in the controller as indicated in Fig. 8 to determine when the drive is approaching zero speed using the inverter switch commutation frequency as input. This information is then used by the PLA interface logic to control drive quadrant changes during speed reversals.

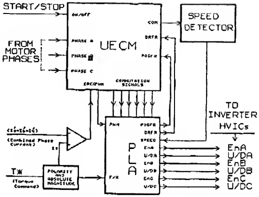

Fig. 8. Block diagram of the sensorless controller.

5. Experimental Results

The assembled four-quadrant drive described above was coupled to a 0.5 hp 12-pole ECM for dynamometer testing. Steady-state regeneration was obtained by using the load machine as a motor to rotate the ECM at fixed speed. The drive has been successfully operated as both a motor and generator over a speed range from -1500 to +1500 r/min.

Figure 9 shows a typical current waveform for Phase A of the ECM during motoring operation. The lower trace in this figure shows the gate drive signal for the lower inverter power switch (S4) associated with Phase A. Note that this switch is pulse-width-modulated only during the second 60 degree interval, consistent with the sequencing scheme shown in Fig. 4. The PWM frequency was set at 10 kHz, yielding the well-regulated current waveform shown in Fig. 9.

Figure 10 shows a comparable current waveform in Phase A during steady-state regenerative operation, together with the S4 gating signal. The presence of PWM switching during the full 120 degree conduction interval is clearly evident in the lower trace. In addition, the amplitude of the current ripple during regenerative operation is visibly higher than during motoring operation under similar speed conditions, consistent with the predictions of Fig. 7. Despite the higher ripple, the current waveform is still well-behaved in all regards.

Finally, Fig. 11 shows several of the key drive waveforms during a speed reversal. The current limit in the drive, which limits the available accelerating and decelerating torque, has been set at 1.4 Amps. The upper most trace in Fig. 11 is the rectified speed signal developed by the speed detector block noted in Fig. 8. The change of state of the DRFR logic signal at the bottom of Fig. 11 marks the initiation of the speed reversal command when braking torque is commanded. The drive responds by decelerating to zero speed, at which time the n_{min}

Fig 9 Typical phase current and lower switch gate drive signal for phase A (PWM frequency = 10kHz, I* = 1.0 Amp, n = 426 r/min) during motoring.

Fig. 10. Typical phase current and lower gate drive signal for phase A (PWM frequency 10kHz, I* = 1.0 Amp, n = 426 r/min) during regeneration.

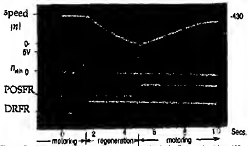

Fig. 11. Oscillogram showing a transition from motoring in the first quadrant (n = 430 rpm, I* = 1.4 Amp.) to motoring in the third quadrant (n = -430 rpm, I* = 1.4 Amp). The motor is decelerated to near zero speed (n_{min} signal high level) and then accelerated to the new operating point in the third quadrant.

zero-speed detector signal shown in the middle of Fig. 11 goes high momentarily, providing the necessary conditions for the drive to change to motoring operation in the reverse direction. This speed reversal is marked by the change in state of the POSFR command. The ECM then accelerates to its final speed as shown on the right side of Fig. 11.

6. Conclusions

The new "sensorless" ECM drive configuration presented in this paper incorporates the following key features:

1) Elimination of discrete position sensors by means of indirect rotor position sensing using the motor back-EMF voltages.
2) Elimination of all discrete current sensors in favor of current sensors integrated into the six MOS-gated inverter power switches.
3) High-quality current regulation and torque control achieved in all operating modes using the incomplete current feedback information provided by the integrated current sensors.
4) Full four-quadrant drive operation, including regeneration back to the DC input power bus.
5) Drive parts minimization achieved by means of a custom-VLSI drive control chip combined with HVIC gate drive chips, compatible with ECM drive ratings from fractional to at least 10 hp.

Acknowledgment

This work was performed using facilities at both GE Corporate R&D in Schenectady, NY, and at Texas A&M University in College Station, TX. The availability of a university grant from GE to partially support this work is gratefully acknowledged.

References

[1] K. Iizuka, et al., "Microcomputer Control for Sensorless Brushless Motor", IEEE Transactions on Industry Applications, Vol. IA-21, No. 4, May/June 1985, pp. 595 - 601.
[2] "Sensorless Spindle Motor Controller", Part ML4410, Advance Information, Microlinear Corporation, Jan. 1990.
[3] United States Patent No. 4,169,990, "Electronically Commutated Motor", granted to General Electric Company, Inventor: D. Erdman, October 2, 1979.
[4] T.M. Jahns, R.C. Becerra, and M. Ehsani, "Integrated Current Regulation for a Brushless ECM Drive". IEEE Transactions on Power Electronics, Vol. 6, No. 1, Jan. 1991.
[5] D. M. Erdman, H. B. Harms, and J. L. Oldenkamp, "Electronically Commutated DC Motors for the Appliance Industry", Conf. Record of 1984 IEEE Industry Application Society Annual Meeting, pp. 1339-1345.
[6] T.J.E. Miller, Brushless Permanent Magnet and Reluctance Motor Drives, Oxford Science Publications, Clarendon Press, Oxford, 1989.
[7] T.M. Jahns, "Torque Production in Permanent Magnet Synchronous Motor Drives with Rectangular Current Excitation", IEEE Trans. on Industry Applications, Vol. IA-20, No. 4, July/Aug. 1984, pp. 803-813.
[8] R.C. Becerra, M. Ehsani, and T.M. Jahns, "Four-Quadrant Brushless ECM Drive with Integrated Current Regulation, Conf. Record of 1989 IEEE Industry Applications Society Annual Meeting, San Diego, pp. 819-828.
[9] J.G. Mansmann, E.J. Wildi, J.R. Walden, K. Fujino, and Y. Hasegawa, "Flexible High-Voltage Half-H Bridge Motion Controller/Driver", Power Conversion & Intelligent Motion, May 1988, pp. 54-62.